CHEMISTRY
A EUROPEAN JOURNAL

DOI: 10.1002/chem.201001679

A Highly Efficient and Extensively Reusable "Dip Catalyst" Based on a Silver-Nanoparticle-Embedded Polymer Thin Film

E. Hariprasad and T. P. Radhakrishnan*[a]

Abstract: Achieving a harmonious combination of the efficiency of homogeneous catalysts with the reusability of heterogeneous catalysts is a fundamental and challenging problem. Metal nanoparticles in a suitable matrix offer a potential solution. However an ideal design is yet to be realized, because the critical requirements of facile access to the catalyst, its durability, and ease of retrieval and reuse are difficult to reconcile. We report herein a multilayer free-standing thin-film catalyst based on silver nanoparticles, generated in situ inside poly(vinyl alcohol) by using a facile protocol, which shows excellent efficiency and extensive reusability in the prototypical reaction, the reduction of 4-nitrophenol by sodium borohydride. The "dip catalyst" film, which can start/stop the reaction instantaneously by mere insertion/removal, is used 30 times leading to a total turnover number (TON) of ≈3390, which is unprecedented for this reaction. The efficiency of the catalyst is reduced only marginally at the end of these runs, promising further extended usage. The unique advantage of convenient catalyst monitoring is illustrated by the periodic spectroscopic and microscopic examinations of the thin film, which revealed the basis of its durability. The demonstrated potential of metal-nanoparticle-embedded polymer thin films, coupled with their versatility and ease of fabrication, promises extensive applications in chemical catalysis.

Keywords: heterogeneous catalysis · homogeneous catalysis · nanoparticles · silver · thin films

Introduction

The reusability of a catalyst and hence its efficacy are, in principle limitless, as by definition, it undergoes no transformation itself while promoting a chemical reaction. However, due to several constraints, including chemical instability and physical loss, such potentials are rarely realized. Metal nanoparticles are efficient catalysts for a number of reactions, their large surface area to volume ratio and specific surface structure being key factors.[1] They are potential candidates for addressing the fundamental issue of unifying and harnessing the benefits of homogeneous and heterogeneous catalysis.[2,3] In addition to their efficiency and selectivity in enhancing reaction rates,[4] an aspect that makes a catalyst genuinely superior is the feasibility and ease of multiple reuse. Monitoring a nanocatalyst through reuse cycles to assess problems like leaching or shape/size alteration is extremely valuable in the optimization of catalyst design. Even though metal nanoparticle catalysts encapsulated in, or supported on, a wide range of host structures have been explored,[3,5] efficient reuse and catalyst monitoring remain major challenges. We envisaged that polymer thin films with in situ generated metal nanoparticles would be a class of easily fabricated, efficient, and reusable catalysts; that catalyst separation would be trivial, and the thin film would be amenable to convenient examination between uses. Even though metal nanoparticles in polymer membranes have been used in sorption-diffusion-based separations and catalysis,[6] major issues, such as extensive reuse and efficient catalyst monitoring, have not been addressed.

Polymer thin films with embedded metal nanoparticles combine the versatility of the former with the unique properties of the latter. These nanocomposites find applications in several areas, including electronics, photonics, sensors, and medicine.[7–13] Thin films of the nanocomposites can be grown by plasma deposition methods.[7] Various soft chemical routes have also been developed for their fabrication;[12,14–17] in situ growth of metal nanoparticles within a polymer film is especially efficient.[12,15–17] A general protocol that we have optimized involves spin coating a solution

[a] E. Hariprasad, Prof. T. P. Radhakrishnan
School of Chemistry, University of Hyderabad
Hyderabad, 500 046 (India)
Fax: (91) 40-2301-2460
E-mail: tprsc@uohyd.ernet.in

Supporting information for this article is available on the WWW under http://dx.doi.org/10.1002/chem201001679.

of the polymer and the metal precursor onto a substrate followed by thermal in situ reduction of the metal ions to atoms by the polymer itself, which leads to the formation of nanoparticles inside the film.[12,18–20] This methodology is environmentally benign, since the medium used is mostly aqueous, and the potentially toxic[21] nanoparticles are never exposed. Other advantages of the approach include the convenience of monitoring the in situ formation of the metal nanoparticles,[20] even in real time,[22] and the feasibility of fabricating both free-standing films amenable to direct imaging and multilayer films for specific applications.[23] We have demonstrated efficient optical power limiting[18,23] and microwave absorption[24] in silver poly(vinyl alcohol) (Ag–PVA) films. These films have also been used to fabricate high-resolution negative-tone resists,[9] random lasers with coherent feedback,[10] polarizing filters,[25] and a prototype for a generic memory device.[11]

The efficacy of a metal-nanoparticle-embedded thin-film catalyst is best demonstrated by using a well-studied nanoparticle-catalyzed reaction as a benchmark; we chose to investigate the reduction of 4-nitrophenol (4NP) by sodium borohydride. Several metal nanoparticles, including those of palladium, gold, and silver, have been used as catalysts for this reaction.[26–29] The use of silver nanoparticles and host matrices to facilitate catalyst retrieval[30,31] is advantageous in terms of the cost factor; catalysts in the form of powders are, however, prone to losses during filtration or magnetic separation and washing. Efficient retrieval and recycling of the catalyst, as well as assessment of the catalyst between uses, have rarely been realized in the reported studies. It is also notable that characteristics like turnover number (TON) and turnover frequency (TOF) have been reported only in a few cases.

A critical problem with a catalyst based on metal nanoparticles in a polymer thin film (or any other matrix) is the effective reconciliation of conflicting issues such as the durability of the nanocatalyst in the film matrix and facile access of the reactants to the catalyst. We have investigated the efficacy of an Ag–PVA thin film, fabricated by using our methodology, in catalyzing the $NaBH_4$ reduction of 4NP. A multilayer structure, Ag–PVA/PVA/Ag–PVA is shown to provide robust free-standing films with excellent catalytic efficiency. Choice of a polymer with optimal characteristics and the multilayer design facilitate reversible swelling in the aqueous reaction medium, ensuring easy passage of reactants to the catalyst embedded in the polymer matrix without leaching or degradation of the catalyst. In situ monitoring of the reaction kinetics is facile with no interference from the catalyst; high rate constants are observed. Experiments carried out on larger scales establish the high TON and TOF that can be achieved. The catalyst can be reused extensively; 30 runs demonstrated in this study yield an unprecedented total TON of 3395. There is only a marginal reduction in the efficiency of the catalyst after 30 runs, which is promising for further extended usage. Periodic monitoring of the catalyst film unambiguously establishes its stability and durability. Because the catalyst film is removed cleanly at the end of the reaction, workup of the products is convenient. Comparison of the Ag–PVA catalyst with the silver-nanoparticle systems reported earlier for the same reaction, coupled with its ease of fabrication, demonstrates the significant benefits of using metal-nanoparticle-embedded polymer thin films in chemical catalysis. We call them "dip catalysts"[32] to highlight their mode of deployment and ease of reuse. The relevance of this term is accentuated by the fact that insertion/removal of the film can be used to turn the reaction on/off almost instantaneously.

Results and Discussion

Fabrication and characterization of the catalyst film: Ag–PVA film was prepared according to our previously reported methodology,[12,18] with modifications (see Figure 1a) as described in the Experimental Section. Special attention was paid to factors such as the specific polymer used, optimization of the concentration of silver, and accessibility of the reactant molecules to the catalyst. A relatively high-molecular-weight PVA with nearly complete hydrolysis was employed (PVA with lower molecular weight and lower degree of hydrolysis had been used in the earlier studies[18–20]), so that the heat-treated film was insoluble in the aqueous medium under the ambient temperature conditions used in the reaction. The hydrophilic nature of PVA, however, ensures sufficient swelling in the reaction medium, which in turn facilitates the approach of the reactant molecules to the silver nanoparticles. We have explored a range of Ag/PVA weight ratios (x), temperatures (T), and times (t) of heat treatment of the $AgNO_3$–PVA film to achieve appreciable

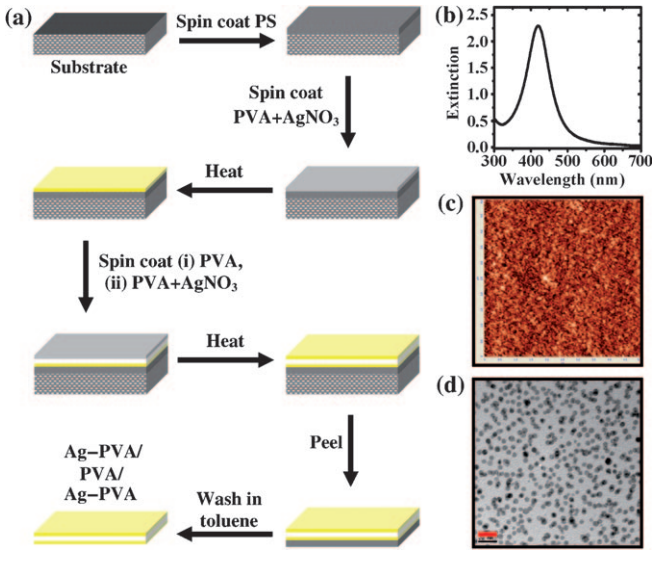

Figure 1. Fabrication and characterization of the Ag–PVA/PVA/Ag–PVA polymer film: a) Schematic representation of fabrication (dimensions not to scale). PS = polystyrene. b) SPR extinction spectrum. c) AFM topography image (5 μm × 5 μm) and d) TEM image (scale bar = 20 nm) of the Ag–PVA film ($x = 0.2$). b) and c) are of the multilayer film and d) of a single-layer film with the same composition.

concentration of relatively small silver nanoparticles; the optimal values determined are $x=0.2$, $T=130\,°C$, and $t=4\,h$; kinetics experiments carried out with films of varying x are discussed below. The film must be sufficiently thick and robust for repeated use in the reaction involving stirring, with washing in between uses. At the same time, efficient utilization of the silver nanoparticles demands that the film is sufficiently thin and that the particles are available close to the film surface. These requirements are reconciled effectively in the design of the multilayer structure with thin active layers (Figure 1a). The thickness of the individual layers was regulated by varying the solution viscosity and spin-coating conditions. Typical values of the thickness of the polystyrene, Ag–PVA (I), PVA, and Ag–PVA (II) layers in the films used in the present studies are around 3.20, 0.19, 1.00, and 0.13 μm, respectively (see Table S1 in the Supporting Information). The characteristic surface plasmon resonance (SPR) extinction of the silver nanoparticles in the multilayer film is shown in Figure 1b. Figure 1c and d show the AFM image of the smooth film surface (average roughness = 0.77 nm) and the TEM image of a single-layered film, respectively. The latter reveals a homogeneous distribution of spherical nanoparticles with an average diameter of around 5.0 nm (see Figure S1 and Table S2 in the Supporting Information).

Kinetic studies and evaluation of TON: We have investigated the kinetics of reduction of 4NP catalyzed by the Ag–PVA film using the setup depicted in Figure 2, which is further described in the Experimental Section. As the reduction by $NaBH_4$ is sluggish, the absorption due to the 4-nitrophenolate remains unaltered if no catalyst is introduced (see Figure S2 in the Supporting Information). However, within a few seconds of introducing the catalyst film (see the Experimental Section for details), the peak begins to decay as reduction of the nitro group starts; a concomitant rise of the peak due to 4-aminophenolate is observed. Figure 3a shows the profile of a typical

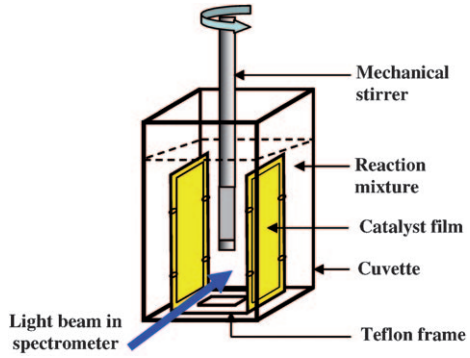

Figure 2. Schematic representation of the setup used in the catalysis studies; the figure shows the catalyst film fixed on a Teflon frame, the mechanical stirrer, the reaction mixture in the cuvette, and the light beam path.

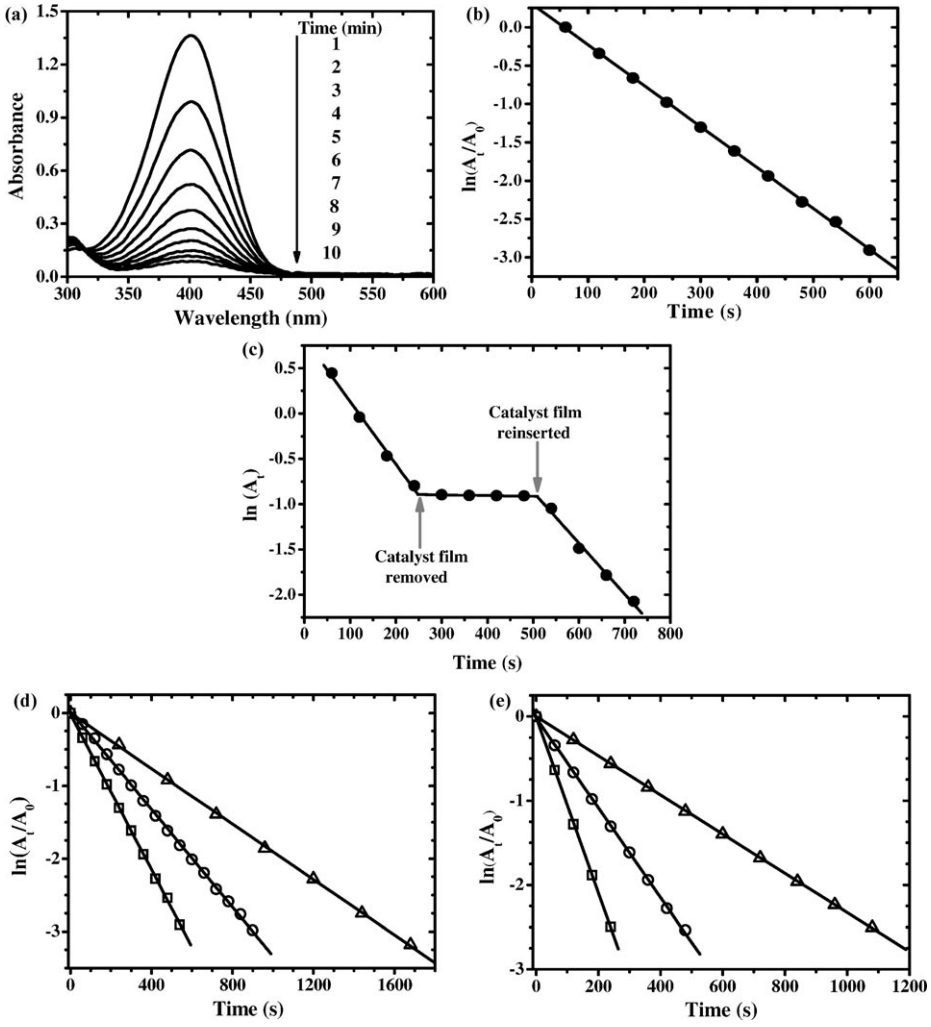

Figure 3. a) Electronic absorption spectra of the reaction mixture ([4NP] = 0.11 mM, [$NaBH_4$] = 11 mM) at 25 °C as a function of time, following the insertion of the Ag–PVA multilayer catalyst film. b) Plot of $\ln(A_t/A_0)$ versus time; A_0 and A_t are the absorbances at 400 nm at time 0 and t, respectively. c) Plot of $\ln(A_t)$ as a function of time, in an experiment in which the catalyst film was removed and reinserted. d) Kinetics plots for three different weight ratios Ag/PVA (x; △: $x=0.05$, ○: $x=0.10$, □: $x=0.20$) of the catalyst film (with [4NP] = 0.11 mM, [$NaBH_4$] = 11 mM). e) Kinetics plots for three different ratios (50 (△), 100 (○), 200(□)) of [$NaBH_4$]/[4NP] (with [4NP] = 0.11 mM, $x=0.2$). The least squares line of best fit is shown in each case; in (c), it is shown for each segment of the data.

run; the peak decays steadily with time. As a large excess of $NaBH_4$ is used, the reaction is expected to be pseudo first order; this is confirmed by the plot in Figure 3b. Note that this procedure, whereby the catalyst film is introduced after the reagents are mixed in solution and stirred for a few minutes, gives rise to a clean first-order reaction profile from time zero, with no evidence of the induction period that was observed in some earlier studies.[26] Switching the reaction off or on by the catalyst film is demonstrated in an experiment in which the catalyst film is removed and reinserted after a brief interval; the prompt response of the reaction is vividly captured in the reaction profile shown in Figure 3c. This observation is strong evidence that there is practically no leaching of silver nanoparticles into the reaction medium; easy workup of the reaction products after withdrawal of the catalyst film is thus ensured. We investigated the dependence of the reaction rate constant on two relevant parameters, the value of x of the catalyst film and the $[NaBH_4]/[4NP]$ ratio in the reaction mixture. The kinetics plots are shown in Figure 3d and e, and the estimated rate constants are listed in Table 1. Based on these observations,

Table 1. Apparent rate constants determined for the reduction of 4NP by $NaBH_4$ at 25°C catalyzed by the Ag–PVA multilayer film, for three different weight ratios of Ag/PVA (x) (with $[NaBH_4]/[4NP]=100$) and three different reactant ratios of $[NaBH_4]/[4NP]$ (with $x=0.2$); relevant plots are shown in Figure 3d and e.

Catalyst/reaction parameter		k_{app} [10^{-3} s^{-1}]
x	0.05	1.9
	0.10	3.4
	0.20	5.3
$[NaBH_4]/[4NP]$	50	2.3
	100	5.3
	200	10.4

we conclude that $x=0.2$ and $[NaBH_4]/[4NP]=100$ are optimal for this catalytic reaction. The pseudo-first-order rate constant is found to vary linearly with the amount of catalyst and with $[NaBH_4]$, as expected (see Figure S3 in the Supporting Information). We also explored the temperature dependence of the catalytic process (see Figure S4 in the Supporting Information). Based on the rate constants determined in the range 298–318 K, the activation energy of the reaction is estimated to be 40.9 kJ mol^{-1}, which is in good agreement with reported values.[31,33]

The efficacy of our dip catalyst was investigated by increasing the scale of the reaction while keeping the catalyst film unchanged ($x=0.2$, silver content = 0.65 μmol) and attempting multiple uses of a single film; the $[NaBH_4]/[4NP]$ ratio of 100 was used in all reactions carried out at the ambient temperature of 25°C. With a stiff limit of 15 min kept for completion of the reaction (>99.9% in the first run), it was found that the film could catalyze the reduction of up to 75 μmol of 4NP in a single run. This implies a high TON of ≥114. The TOF for the reaction catalyzed by the Ag–PVA film is 0.127 s^{-1}, which is, once again a high value when compared with those reported earlier (see Table S3 in the Supporting Information). It is important to note that the fraction of silver atoms on the surface of a nanoparticle with diameter of 5.0 nm is around 0.28 (see page S3 in the Supporting Information) and, because the surface atoms effect the actual catalytic process, the effective TON would really be much higher, around 407.

Catalyst recycling and monitoring: Following these observations, we have explored repeated use of the same catalyst film in multiple reaction runs, each one at the scale of 75 μmol of 4NP. After each run, the film was removed, washed with MilliQ water followed by isopropyl alcohol, and dried under vacuum for 20 min before being inserted into a new reaction setup (Figure 4a). The Ag–PVA film was found to be catalytically active even after 30 runs. When the reaction nears completion, the absorbance of the mixture at 400 nm becomes low enough to be measured, and follows the Beer–Lambert law (see the Experimental Section). It is also found that the reaction continues to follow a first-order rate law (see Figures S5 and S6 in the Supporting Information). Based on these observations we have estimated the yield of the reaction at 15 min in each run; Figure 4b shows that it decreases only nominally from 99.9 to 95.3% over 30 cycles of use of the same film. This implies that the reaction rate is only slightly reduced after multiple reuses.

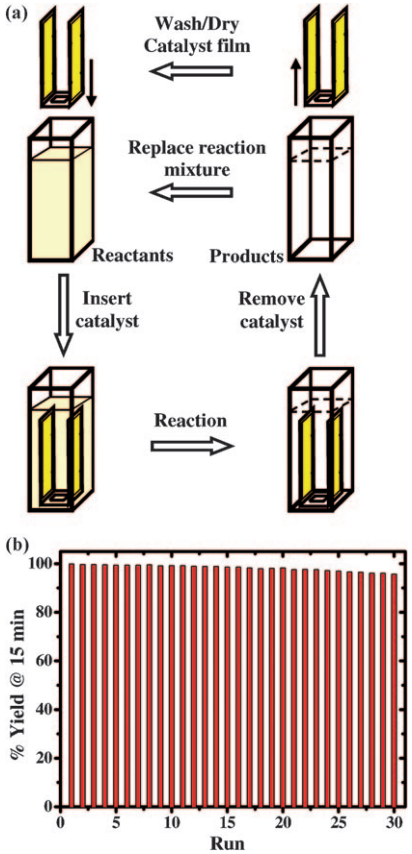

Figure 4. a) Schematic representation of the reuse cycle of the dip catalyst. b) Reaction yield at 15 min for the reduction of 4NP by $NaBH_4$ at 25°C ($[4NP]=0.03$ M, $[NaBH_4]=3.0$ M, volume of reaction mixture = 2.5 mL), in repeated runs catalyzed by the same Ag–PVA multilayer film.

Note that the highest number of repeated uses reported earlier for this catalytic reaction is 21, which was achieved with an Ag/Fe_2O_3 catalyst.[31] In that case, catalyst removal was carried out by using a magnet, and the catalytic activity showed an abrupt decline at the end of 21 runs. Our catalyst film, on the contrary, is easy to remove and reinstall in a new reaction setup, and continues to be quite active after 30 runs. As we have used the same catalyst through all of the runs, the total TON at the end of 30 runs amounts to the very high value of 3395 (based on the yield at 15 min in each case). The highest TONs for the silver-nanoparticle-catalyzed reduction of 4NP with $NaBH_4$ estimated from literature data are 515 (achieved by using a polymer-nanocapsule-based catalyst[26]) and 660 (achieved over 21 runs with the Ag/Fe_2O_3 catalyst[31]). A detailed comparison of the performance of the Ag–PVA multilayer film relative to silver-nanoparticle-based catalyst systems reported earlier for the reduction of 4NP by $NaBH_4$ is provided in Table S3 in the Supporting Information; the superior efficiency and reusability of our new dip catalyst is clearly evident.

Compared to the various forms in which metal nanoparticles have been used as catalysts, the nanocomposite polymer thin film offers critical advantages not only in terms of convenient reuse as shown above, but also in terms of easy monitoring of the catalyst between the reuses. We have examined the Ag–PVA multilayer film at regular intervals through the reuse cycles by using microscopy and spectroscopy. AFM images of a film recorded between repeated uses are shown in Figure 5a; the morphology is largely preserved and the surface roughness nearly constant throughout, which reflects the stability and durability of the film. The intensity of the SPR extinction of the film also remains nearly constant through the 30 reaction runs (Figure 5b), which indicates, once again, negligible leaching of the silver nanoparticles. There is a small (ca. 10 nm) blueshift of the absorption peak after the first use of the film. Subsequently, the spectral position and shape remain consistent throughout, except for a very small increase of the baseline near 550 nm. The TEM images of the film through the multiple reuses (Figure 5c) provide useful insight into these observations and the status of the catalyst nanoparticles. The film used in the reaction medium is found to have a slightly broader distribution of nanoparticle sizes, including some smaller ones, than the fresh film. While the average sizes of the nanoparticles show very little variation, the number of nanoparticles observed in a unit area of the film, as well as their total surface area, decrease slightly over repeated uses (see Figure S1 and Table S2 in the Supporting Information). The formation of smaller particles (which results in the blueshift of the SPR peak) and minor aggregation effects (reflected in the baseline shift) are possibly induced by the slight dissolution/reformation of the nanoparticles effected by the reaction medium with high concentration of $NaBH_4$. As the changes in the nanoparticles are quite small, the impact on catalyst efficiency is marginal.

We also explored the possibility of using the catalyst film for a single run on a mmol scale: 1 mmol of 4NP and 100 mmol of $NaBH_4$ were used in the reaction, in which the concentration of 4NP was maintained as in earlier runs. As the volume of solution was now larger, the film was suspended in the reaction mixture, which was stirred using a magnetic bar. After the strong yellow color had mostly disappeared, completion of the reaction was detected by recording the electronic absorption spectrum of aliquots of the reaction mixture. It was found that 95% of the reaction was completed in around 3.5 h, which implied a TON of 1461 and TOF of 0.116 s^{-1} achieved in a single run.

The various experiments described above attest to the robustness and efficiency of the Ag–PVA thin-film catalyst. The fact that the film effects efficient catalysis over several rounds of reaction and on a relatively large scale suggests that the nanoparticles are accessible to the reactant molecules throughout, but retain their integrity through repeated uses. The crucial role of the polymer matrix in channeling the reactants to the catalyst and the products away is clearly

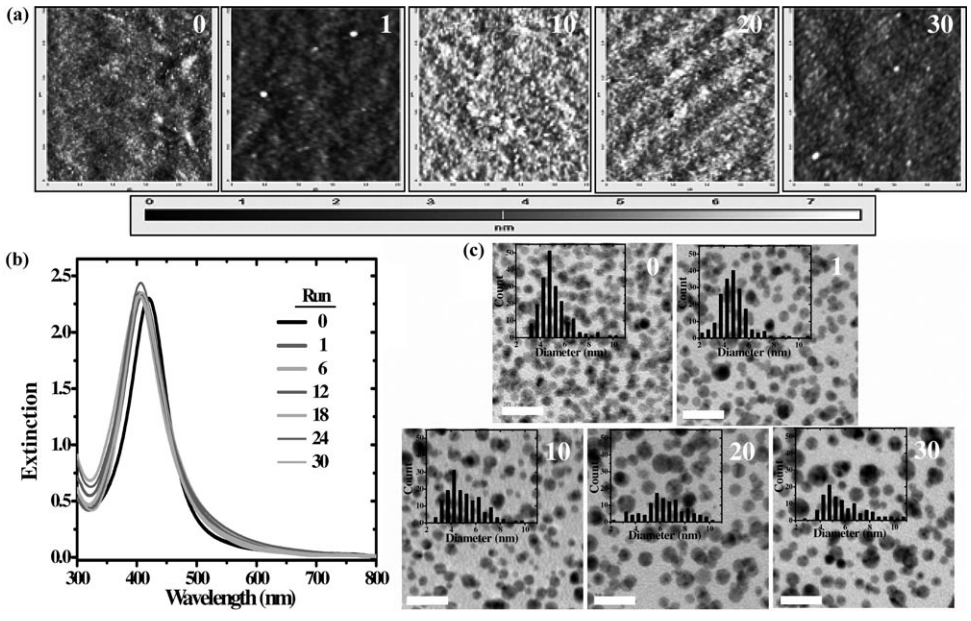

Figure 5. Monitoring the dip catalyst during the reuse cycles: a) AFM topography images (2.5 μm × 2.5 μm, height scale is shown beneath the images) of an Ag–PVA multilayer film catalyst through repeated runs of the reduction of 4NP by $NaBH_4$ ([4NP] = 0.03 M, [$NaBH_4$] = 3.0 M, volume of reaction mixture = 2.5 mL); the run number is indicated on the images, the zeroth run corresponds to the fresh film. b) SPR extinction of one Ag–PVA multilayer film catalyst through repeated runs of the reaction. c) TEM images of a single-layer Ag–PVA film through repeated runs of the reaction; scale bar = 20 nm; particle-size distributions are shown.

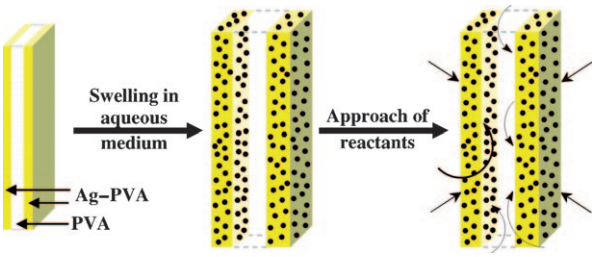

Figure 6. Schematic representation of the swelling of the Ag–PVA/PVA/Ag–PVA catalyst film in the aqueous reaction medium, and the facile approach of the reactants to the silver nanoparticles (shown as black dots) embedded in the Ag–PVA layers.

significant. The plausible mechanism of action of the multilayered polymer-film catalyst is depicted in Figure 6. In aqueous medium, the PVA matrix swells to allow admission of the solution into the film; optical micrographs and AFM images of the films demonstrate this clearly (see Figure S7 in the Supporting Information). The reactant molecules have unhindered access to the metal nanoparticles from the outer surfaces of the multilayer film as well as through the middle layer of pure PVA, which enhances the catalytic activity. The minor decline observed in the rate of the reaction with increasing reuses may be due to the nanoparticles migrating deeper into the polymer matrix as a result of repeated swelling and drying cycles, or small changes occurring in the size distribution. The nature of the polymer and the multilayer structure are indeed critical to the efficient functioning of the catalyst system.

Conclusion

The present study demonstrates the unique advantages of metal-nanoparticle-embedded polymer thin film as a superior catalyst system that mediates reactions effectively while retaining its integrity. A simple multilayer-film design was developed, and a convenient protocol for its fabrication through in situ formation of silver nanoparticles inside PVA film was optimized. The kinetics of the catalytic reaction was investigated, and optimal catalyst composition and reactant ratio determined. The thin-film catalyst was shown to produce a TON of 114 in a single reaction run that lasted around 15 min. Retrieval and reintroduction of the thin-film dip catalyst are easy to implement, providing a simple mechanical control of the reaction. The same catalyst film can be reused more than 30 times, which leads to a total TON of around 3390. The cheap materials and simple methods used in catalyst fabrication, in combination with the large TON achieved, establish the cost effectiveness of the present approach. Spectroscopy and microscopy were used to monitor the catalyst film during the repeated usage, and demonstrate the basis of its durability and stability. Embedding the metal nanoparticles inside the polymer film effectively precludes aggregation, and enables long-term storage of these nanocomposite films, an aspect of considerable practical relevance. The present study illustrates the promise of metal-nanoparticle-embedded polymer thin films as versatile and effective catalysts. The wide range of metal–polymer combinations that can be exploited, and the plethora of reactions that can be addressed, point to the enormous potential of the general approach developed herein.

Experimental Section

Fabrication of the catalyst film: The fabrication protocol is shown schematically in Figure 1a. The glass substrate for coating the film was cleaned by washing and ultrasonicating in isopropyl alcohol, and then dried. A few drops of a solution of polystyrene (Aldrich, average molecular weight = 280 kDa) in toluene (1 g in 8 mL) was spin coated by using a Laurell Technologies Corporation Model WS-400B-6NPP/LITE/8K photoresist spinner operated at 1000 RPM for 10 s, and dried in a hot-air oven at 90 °C for 15 min. Aqueous (Millipore MilliQ water, resistivity = 18.2 MΩ cm) solutions of $AgNO_3$ (Aldrich, purity = 99.9+ %) and PVA (Aldrich, average molecular weight = 85–146 kDa, hydrolysis = 99+ %) were mixed in required proportions; for example, $AgNO_3$ (63 mg) dissolved in water (2 mL) was mixed with PVA (200 mg) dissolved in water (4 mL) to prepare a film with an Ag/PVA weight ratio of 0.2. The solution was spin coated at 500 RPM for 10 s followed by 6000 RPM for 10 s onto the polystyrene layer. After heating at 90 °C for 30 min, an aqueous solution of PVA was spin coated at 500 RPM for 10 s followed by 2000 RPM for 10 s and dried in a hot air oven at 90 °C for 30 min. The final layer was formed by spin coating the $AgNO_3$–PVA solution as before; the resulting multilayer film was then heated at 130 °C for 4 h. The extended heating ensures complete reduction of the Ag^+ ions as well as stability of the film in aqueous medium. The film was peeled off the glass substrate and the polystyrene layer removed by washing in toluene to obtain the free-standing Ag–PVA/PVA/Ag–PVA film.

Characterization of the catalyst film: The film was weighed accurately after coating each layer. The final content of Ag was estimated based on the Ag/PVA ratio used in the initial solution mixture, assuming complete reduction of the Ag^+ ions; this assumption is justified by the observation of saturation of the SPR extinction under the fabrication conditions (see Figure S8 in the Supporting Information). Film thickness was measured by using an Ambios Technology XP-100 Profilometer. Electronic spectra were recorded on a Varian Model Cary 100 UV/Vis spectrometer. AFM imaging was carried out on an NT-MDT model Solver Pro M AFM by using a 3 μm scanner in contact mode. In addition to the freshly fabricated film, small pieces cut from the same catalyst film after various numbers of uses in the reaction were imaged. Swelling of the three-layer film on absorption of water was examined by using a WITec model Alpha300 R AFM, imaging with a 100 μm scanner in contact mode, and recording optical micrographs with a 10× objective lens. TEM was carried out by using a TECNAI G2 FEI F12 TEM at an accelerating voltage of 200 kV. Samples for TEM were prepared by using our previously developed technique.[18] As the multilayer film is too thick for direct imaging, a single layer of $AgNO_3$–PVA (with the same composition as that of the catalyst film) was coated onto a polystyrene-coated glass and annealed at 130 °C for 4 h. The film was peeled and placed on a 200 mesh copper grid and the polystyrene dissolved by dipping in toluene. The Ag–PVA film sticking to the grid was imaged directly. The catalyst content estimated by using the TEM images is in good agreement with that determined by weighing (see page S3 in the Supporting Information). One such film was placed in a the reaction system in a Petri dish for the time corresponding to each run in the catalytic studies for up to 30 runs. Small pieces cut from this film after various numbers of uses were imaged.

Catalysis studies: Silver-nanoparticle-catalyzed reduction of 4NP by $NaBH_4$ was monitored by using the electronic absorption of the reaction mixture as a function of time. A standard polystyrene cuvette (4.5 mL, 1 cm path length) was used. For the kinetics studies, an aqueous solution of 4NP (3.0 mL, 0.12 mM) was placed in the cuvette, and $NaBH_4$ (aqueous solution, 0.2 mL, 0.18 M) was added (final concentrations: [4NP] = 0.11 mM, [$NaBH_4$] = 11 mM), whereupon the yellow coloration deepened

due to the formation of 4-nitrophenolate; the absorption has λ_{max} of around 400 nm (see Figure S9 in the Supporting Information). The solution was stirred for 6 min. The catalyst film (thickness ca. 1.3 μm, total surface area = 35 cm^2, total weight = 0.42 mg; page S3, Supporting Information) fixed on a Teflon frame was introduced in such a way that the light beam was transmitted freely through the solution (Figure 2). The reaction mixture was stirred with a glass/Teflon mechanical stirrer introduced from the top, and ending just above the light beam path. The absorption spectrum was recorded at regular intervals to monitor the decay of the peak due to the reduction of 4-nitrophenolate. Similar experiments were carried out on a larger scale by using 4NP (1.0 mL, 75 mM) and $NaBH_4$ (1.5 mL, 5.0 M solution) (final concentrations, [4NP] = 0.03 M, [$NaBH_4$] = 3.0 M) to determine the TON of the catalytic process. Since the concentration of 4-nitrophenolate is high, the absorbance is beyond measurement limits at the beginning of the reaction. However, when the reaction nears completion, the absorbance is measurable. We have verified the adherence to Beer–Lambert law in these ranges (see Figure S6 in the Supporting Information), and the exact concentrations were estimated from the absorbance values.

Details of microscopy, spectroscopy, kinetic studies, thin-film characterization, and survey of earlier reports on silver-nanoparticle-catalyzed reduction of 4-nitrophenol by sodium borohydride can be found in the Supporting Information.

Acknowledgements

Financial support from the Department of Science and Technology, New Delhi and infrastructure support from the Centre for Nanotechnology at the University of Hyderabad are acknowledged with gratitude. We thank Mr. M. Durga Prasad and Mr. E. Manohar Reddy for help with the TEM imaging. E.H. thanks CSIR, New Delhi for a senior research fellowship.

[1] a) M. Moreno-Mañas, R. Pleixats, *Acc. Chem. Res.* **2003**, *36*, 638; b) R. Narayanan, M. A. El-Sayed, *J. Am. Chem. Soc.* **2004**, *126*, 7194; c) C. Burda, X. Chen, R. Narayanan, M. A. El-Sayed, *Chem. Rev.* **2005**, *105*, 1025; d) *Nanocatalysis* (Eds.: U. Heiz, U. Landman), Springer, Berlin, **2007**; e) G. A. Somorjai, J. Y. Park, *Top. Catal.* **2008**, *49*, 126.

[2] C. A. Witham, W. Huang, C. Tsung, J. N. Kuhn, G. A. Somorjai, F. D. Toste, *Nat. Chem.* **2010**, *2*, 36.

[3] a) G. Schmid, *Chem. Rev.* **1992**, *92*, 1709; b) A. Roucoux, J. Schulz, H. Patin, *Chem. Rev.* **2002**, *102*, 3757; c) S. Shylesh, V. Schünemann, W. R. Thiel, *Angew. Chem.* **2010**, *122*, 3504; *Angew. Chem. Int. Ed.* **2010**, *49*, 3428.

[4] F. Zaera, *J. Phys. Chem. Lett.* **2010**, *1*, 621.

[5] a) R. M. Crooks, M. Zhao, L. Sun, V. Chechik, L. K. Yeung, *Acc. Chem. Res.* **2001**, *34*, 181; b) J. Kim, A. A. Gewirth, *J. Phys. Chem. B* **2005**, *109*, 9684; c) H. Song, R. M. Rioux, J. D. Hoefelmeyer, R. Komor, K. Niesz, M. Grass, P. D. Yang, G. A. Somorjai, *J. Am. Chem. Soc.* **2006**, *128*, 3027; d) S. Wang, X. He, L. Song, Z. Wang, *Synlett* **2009**, 447; e) H. Jiang, B. Liu, T. Akita, M. Haruta, H. Sakurai, Q. Xu, *J. Am. Chem. Soc.* **2009**, *131*, 11302.

[6] a) S. S. Ozdemir, M. G. Buonomenna, E. Drioli, *Appl. Catal. A* **2006**, *307*, 167; b) N. B. McKeown, P. M. Budd, *Chem. Soc. Rev.* **2006**, *35*, 675.

[7] a) A. Heilmann, *Polymer Films with Embedded Metal Nanoparticles*, Springer, Berlin, **2003**; b) F. Faupel, V. Zaporojtchenko, H. Greve, U. Schürmann, V. S. K. Chakravadhanula, Ch. Hanisch, A. Kulkarni, A. Gerber, E. Quandt, R. Podschun, *Contrib. Plasma Phys.* **2007**, *47*, 537.

[8] a) W. Caseri, *Macromol. Rapid Commun.* **2000**, *21*, 705; b) A. L. Stepanov, *Tech. Phys.* **2004**, *49*, 143.

[9] R. Abargues, J. Marqués-Hueso, J. Canet-Ferrer, E. Pedrueza, J. L. Valdés, E. Jiménez, J. P. Martínez-Pastor, *Nanotechnology* **2008**, *19*, 355308.

[10] X. Meng, K. Fujita, Y. Zong, S. Murai, K. Tanaka, *Appl. Phys. Lett.* **2008**, *92*, 201112.

[11] W. L. Leong, P. S. Lee, A. Lohani, Y. M. Lam, T. Chen, S. Zhang, A. Dodabalapur, S. G. Mhaisalkar, *Adv. Mater.* **2008**, *20*, 2325.

[12] G. V. Ramesh, S. Porel, T. P. Radhakrishnan, *Chem. Soc. Rev.* **2009**, *38*, 2646.

[13] P. Zijlstra, J. W. M. Chon, M. Gu, *Nature* **2009**, *459*, 410.

[14] Z. H. Mbhele, M. G. Salemane, C. G. C. E. van Sittert, J. M. Nedeljković, V. Djoković, A. S. Luyt, *Chem. Mater.* **2003**, *15*, 5019.

[15] a) B. C. Sih, M. O. Wolf, *Chem. Commun.* **2005**, 3375; b) M. Sangermano, Y. Yagci, G. Rizza, *Macromolecules* **2007**, *40*, 8827.

[16] a) J. Won, K. J. Ihn, Y. S. Kang, *Langmuir* **2002**, *18*, 8246; b) A. S. Korchev, M. J. Bozack, B. L. Slaten, G. Mills, *J. Am. Chem. Soc.* **2004**, *126*, 10; c) J. Li, K. Kamata, S. Watanabe, T. Iyoda, *Adv. Mater.* **2007**, *19*, 1267; d) S. Horiuchi, Y. Nakao, *Curr. Nanosci.* **2007**, *3*, 206; e) T. Hasell, L. Lagonigro, A. C. Peacock, S. Yoda, P. D. Brown, P. J. A. Sazio, S. M. Howdle, *Adv. Funct. Mater.* **2008**, *18*, 1265.

[17] a) W. Fritzsche, H. Porwol, A. Wiegand, S. Bornmann, J. M. Köhler, *Nanostruct. Mater.* **1998**, *10*, 89; b) S. Rifai, C. A. Breen, D. J. Solis, T. M. Swager, *Chem. Mater.* **2006**, *18*, 21; c) L. Shang, Y. Wang, L. Huang, S. Dong, *Langmuir* **2007**, *23*, 7738; d) J. Zhang, Y. Gao, R. A. Alvarez-Puebla, J. M. Buriak, H. Fenniri, *Adv. Mater.* **2006**, *18*, 3233; e) R. D. Deshmukh, R. J. Composto, *Chem. Mater.* **2007**, *19*, 745.

[18] S. Porel, S. Singh, S. S. Harsha, D. N. Rao, T. P. Radhakrishnan, *Chem. Mater.* **2005**, *17*, 9.

[19] S. Porel, S. Singh, T. P. Radhakrishnan, *Chem. Commun.* **2005**, 2387.

[20] S. Porel, N. Hebalkar, B. Sreedhar, T. P. Radhakrishnan, *Adv. Funct. Mater.* **2007**, *17*, 2550.

[21] P. V. Asharani, G. L. K. Mun, M. P. Hande, S. Valiyaveettil, *ACS Nano* **2009**, *3*, 279.

[22] G. V. Ramesh, B. Sreedhar, T. P. Radhakrishnan, *Phys. Chem. Chem. Phys.* **2009**, *11*, 10059.

[23] S. Porel, N. Venkatram, D. N. Rao, T. P. Radhakrishnan, *J. Appl. Phys.* **2007**, *102*, 033107.

[24] G. V. Ramesh, K. Sudheendran, K. C. J. Raju, B. Sreedhar, T. P. Radhakrishnan, *J. Nanosci. Nanotechnol.* **2009**, *9*, 261.

[25] M. Bernabò, A. Pucci, F. Galembeck, C. A. de Paula Leite, G. Ruggeri, *Macromol. Mater. Eng.* **2009**, *294*, 256.

[26] Y. Gao, X. Ding, Z. Zheng, X. Cheng, Y. Peng, *Chem. Commun.* **2007**, 3720.

[27] a) Y. Lu, Y. Mei, M. Schrinner, M. Ballauff, M. W. Möller, J. Breu, *J. Phys. Chem. C* **2007**, *111*, 7676; b) M. H. Rashid, T. K. Mandal, *J. Phys. Chem. C* **2007**, *111*, 16750; c) A. Murugadoss, A. Chattopadhyay, *Nanotechnology* **2008**, *19*, 015603; d) A. Wang, H. Yin, H. Lu, J. Xue, M. Ren, T. Jiang, *Langmuir* **2009**, *25*, 12736; e) Y. Khalavka, J. Becker, C. Sönnichsen, *J. Am. Chem. Soc.* **2009**, *131*, 1871; f) J. Zeng, Q. Zhang, J. Chen, Y. Xia, *Nano Lett.* **2010**, *10*, 30.

[28] a) S. Oh, M. Kim, S. Choi, J. Chun, K. Lee, A. Gopalan, C. Hwang, K. Sang-Ho, O. J. Hoon, *J. Ind. Eng. Chem.* **2008**, *14*, 687; b) J. Huang, S. Vongehr, S. Tang, H. Lu, J. Shen, X. Meng, *Langmuir* **2009**, *25*, 11890.

[29] a) K. Esumi, R. Isono, T. Yoshimura, *Langmuir* **2004**, *20*, 237; b) Z. Liu, X. Wang, H. Wu, C. Li, *J. Colloid Interface Sci.* **2005**, *287*, 604; c) D. M. Dotzauer, S. Bhattacharjee, Y. Wen, M. L. Bruening, *Langmuir* **2009**, *25*, 1865; d) S. Wunder, F. Polzer, Y. Lu, Y. Mei, M. Ballauff, *J. Phys. Chem. C.* **2010**, *114*, 8814.

[30] a) S. Jana, T. Pal, *J. Nanosci. Nanotechnol.* **2007**, *7*, 2151; b) X. Jia, X. Ma, D. Wei, J. Dong, W. Qian, *Colloids Surf. A* **2008**, *330*, 234.

[31] K. S. Shin, J. Choi, C. S. Park, H. J. Jang, K. Kim, *Catal. Lett.* **2009**, *133*, 1.

[32] Reminiscent of the familiar "dip tea" that comes in porous sachets.

[33] N. Pradhan, A. Pal, T. Pal, *Colloids Surf. A* **2002**, *196*, 247.

Received: June 14, 2010
Published online: October 28, 2010

